*Research Article*

INTERNATIONAL JOURNAL OF ADVANCED ROBOTIC SYSTEMS

*International Journal of Advanced Robotic Systems*
May-June 2018: 1–11

DOI: 10.1177/1729881418773204
journals.sagepub.com/home/arx
SAGE

# New approach of sliding mode control for nonlinear uncertain pneumatic artificial muscle manipulator enhanced with adaptive fuzzy estimator

**Ho Pham Huy Anh[1], Cao Van Kien[1], Nguyen Ngoc Son[2] and Nguyen Thanh Nam[3]**

## Abstract

A new enhanced adaptive fuzzy sliding mode control approach is proposed in this article with its good availability for application in control of a highly uncertain nonlinear two-link pneumatic artificial muscle manipulator. Stability demonstration of the robust convergence of the closed-loop pneumatic artificial muscle manipulator system based on a novel enhanced adaptive fuzzy sliding mode control is experimentally proved using Lyapunov stability theorem. Obtained result confirms that the new enhanced adaptive fuzzy sliding mode control method, applied to the two-link uncertain nonlinear pneumatic artificial muscle manipulator system, is fully investigated with better robustness and precision than the standard sliding mode control and fuzzy sliding mode control techniques.

## Keywords

Enhanced adaptive fuzzy sliding mode control, pneumatic artificial muscle actuator, two-link nonlinear uncertain serial PAM manipulator, Lyapunov stability theorem

Date received: 5 April 2017; accepted: 14 March 2018

Topic: Robot Manipulation and Control
Topic Editor: Andrey V Savkin
Associate Editor: Junzhi Yu

## Introduction

Up to now, it is evident to recognize the benefits of sliding mode control (SMC) related to maintain robust to uncertainties and external noises. A SMC approach via its switching rules ensures asymptotic stability of the investigated nonlinear system. Hence SMC has been increasingly applied in numerous industrial applications.[1] Esmaeili et al.[2] and Yang and Kim[3] successfully applied SMC for trajectory tracking of non-holonomic wheeled mobile robots. Shiri and Saeed[4] introduced adaptive SMC for robotic arms with parameter uncertainty. Matveev et al.[5] proposed a new nonlinear SMC of an unmanned agricultural tractor. Sarfraz et al.[6] applied a novel robust stabilizing control of a non-holonomic underwater vehicle system with uncertainties via adaptive integral sliding mode. Unfortunately, the inherent drawback of SMC is related to its switching control issue which causes chattering phenomenon. In order to remove the chattering effect, it is often to add a saturated function[7]

[1] Faculty of Electrical and Electronics Engineering (FEEE), Key Laboratory of Digital Control and System Engineering (DCSELAB), Ho Chi Minh City University of Technology (VNU-HCM), Ho Chi Minh City, Vietnam
[2] Faculty of Electronics Technology, Industrial University of HCM City, Ho Chi Minh City, Vietnam
[3] Key Laboratory of Digital Control and System Engineering (DCSELAB), Ho Chi MInh City University of Technology, VNU-HCM, Ho Chi Minh City, Vietnam

**Corresponding author:**
Ho Pham Huy Anh, Faculty of Electrical and Electronics Engineering (FEEE), Key Laboratory of Digital Control and System Engineering (DCSELAB), Ho Chi Minh City University of Technology, Ho Chi Minh City University of Technology (VNU-HCM), Ho Chi Minh City, Vietnam.
Email: hphanh@hcmut.edu.vn

within the sliding surface. The disadvantage issued is that this addition can spoil Lyapunov stability of the closed-loop nonlinear plant. As a consequence, traditional SMC method encounters difficulty in controlling unstructured model uncertainties. Recent studies proved that it can partially surpass this difficulty by combining a SMC controller and other intelligent models. Son et al. have successfully identified and controlled the nonlinear dynamic system through combining MDE with adaptive neural model,[8] and Fei et al. did that by combining SMC with recurrent neural structure.[9]

An efficient combination for nonlinear dynamic system control has been introduced between SMC method and fuzzy proportional-integral controllers,[10,11] or between SMC and adaptive fuzzy model.[12–14] The adaptive fuzzy rules in these techniques are implemented to ensure partial satisfaction of the Lyapunov stability. Such initial promising results have inspired for recently proposed hybrid fuzzy SMC (FSMC) methods in which the asymptotic stability of the investigated closed-loop FSMC plant is partly and efficiently demonstrated. Soltanpour et al.[15], Anand and Mary[16], Wang Y and Fei[17], and Ullah et al.[18] applied FSMC in control of driving systems, including brush-less direct current motor,[15,16] permanent magnet synchronous motor,[17] position servo system.[18] Oveisi et al.[19] proposed adaptive FSMC combined with robust observer for uncertain nonlinear system control. Boldbaatar et al.[20] introduced a new self-organizing FSMC for uncertain temperature control. Moussaoui et al.[21] proposed an adaptive FSMC control for under-actuated dynamic system. Fei et al.[22] successfully introduced a new adaptive FSMC controller for micro electro-mechanical systems triaxial gyroscope. In robotic applications, FSMC controllers have been successfully applied in numerous cases. Jiao et al.[23] have applied the adaptive type-2 FSMC for nonlinear hypersonic aircraft system. Li et al.[24] proposed an adaptive SMC combined with an interval type-2 fuzzy system for controlling nonlinear manipulator. Liang et al.[25] successfully applied a new path following control of an under-actuated autonomous underwater vehicle based on fuzzy backstepping sliding mode approach. The advantage of this combination is that the fuzzy rules permit fuzzy systems to approximate arbitrary continuous equations. Furthermore as to approximate a time-varied nonlinear system, a fuzzy set often needs quite many fuzzy rules. Then, the very huge fuzzy rules will require a high time-consuming computation cost.

Nowadays, pneumatic artificial muscle (PAM) manipulator has been increasingly applied in numerous service, health care, and industrial applications. Unfortunately, the drawback related to the uncertain and hysteresis characteristics of PAM actuators has inspired numerous hybrid advanced controllers to efficiently control the PAM-based robotic applications, including the FSMC. Amar et al.[26] successfully applied a decentralized radial basic function neural networks type-2 FMSC controller for robot manipulator driven by artificial muscles. Chang[27] proposed an adaptive self-organizing FSMC controller for a 2-degree of freedom (2-DOF) serial PAM robot. The fact is that such proposed FSMC technique seems too complex to apply in practice and takes more time to compute and unable to attain required precision. Shi et al.[28] proposed the hybrid control for a parallel PAMs manipulator combining SMC and fuzzy cerebellar model articulation controller (CMAC). Nevertheless, this hybrid fuzzy CMAC-SMC approach for PAM manipulator system seems too complex to be applied in industry, and furthermore, the system stability based on Lyapunov stability principle is not yet demonstrated.

Based on the abovementioned results this article introduces a novel enhanced adaptive fuzzy sliding mode control (EAFSMC) approach which will be tested on the highly nonlinear serial PAM robot. The new contributions of this article are as follows:

1. Redesign adaptation laws of algorithm which is initiatively designed for a serial PAM robot and attains more accurate and takes less time to compute than the compared FSMC of serial PAM robot[22] and the comparative hybrid fuzzy CMAC-SMC of parallel PAM manipulator.[23]
2. Initiatively develop the Lyapunov function candidate and mathematically demonstrate the asymptotic convergent stability for the closed-loop serial PAM robot under proposed EAFSMC.
3. Comparatively verify both FSMC algorithms[22,23] and the new advanced EAFSMC algorithm related to two principal concepts: the flexibility of the fuzzy set in use and the results that EAFSMC adaptively and robustly ensures during the control of a highly nonlinear serial PAM robot. Concretely, it comparatively tests the availability of online tuning approach, the number of fuzzy if-then laws installed of the new EAFSMC controller, the tracking precision performance, and the total time-consuming computation criteria, respectively. Moreover, our analysis of the experiment tests will be also focused on chattering attenuation.

The rest of this article is organized as follows. The second section introduces the highly nonlinear serial PAM robot. The third section presents the traditional FSMC and its application to a highly nonlinear serial PAM robot. The fourth section presents the novel proposed EAFSMC approach and demonstrates its stability based on Lyapunov theorem well suited to the serial PAM robot application. The fifth section presents the experiment results of the proposed EAFSMC algorithm applied to the highly nonlinear serial PAM robot system. Eventually, the sixth section contains the conclusion.

## The 2-DOF serial PAM robot set-up

The experimental setup configuration and working principle of the 2-DOF serial PAM robot is shown in Figures 1 and 2.

The experimental configuration of the 2-DOF serial PAM robot is illustrated in Figure 2. The setup includes a

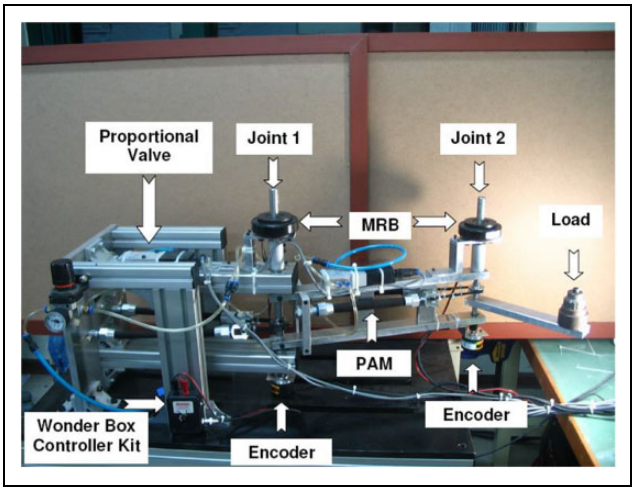


**Figure 1.** Experimental setup configuration of the 2-DOF serial PAM robot. DOF: degrees of freedom; PAM: pneumatic artificial muscle manipulator.

personal computer (PC; Pentium 4.7 GHz) that generates the voltage signals $u_1(t)$ and $u_2(t)$ to control the two proportional valves (MPYE-5-1/8HF-710B [FESTO-Germany]), via a D/A card (PCI 1720 [AdvanTech-Taiwan]) which converts numerical signals from PC to analog voltages, $u_1(t)$ and $u_2(t)$, respectively.

The rotation torque is produced by the pneumatic pressure difference, provided from air compressor, between the antagonistic PAM muscles. Hence, both joints of the 2-DOF serial PAM robot will be rotated to track the required joint angles ($Y_{\mathrm{REF1}}(k)$ and $Y_{\mathrm{REF2}}(k)$), respectively. The joint angles, $\theta_1$ (°) and $\theta_2$ (°), are measured by two rotary encoders (H40-8-3600ZO [Metronix-South Korea]) and sent back to the PC via a 32-bit counter card (PCI QUAD-4 [COMPUTING MEASUREMENT, USA]) which converts pulse signals to joint angle values $y_1(t)$ and $y_2(t)$, respectively. The pneumatic flow is provided under the pressure of 4 bar and the software algorithm of the closed-loop control system is coded in C-mex code run in Real-Time Windows Target tool of MATLAB-SIMULINK (MATLAB@) platform. Table 1 tabulates the configuration of the experimental serial PAM robot setup installed from Figure 2.

## SMC of the 2-DOF Serial PAM robot

The dynamic equation of an $n$-link robotic manipulator is defined as

$$\boldsymbol{M}(\boldsymbol{q})\ddot{q} + \boldsymbol{C}(\boldsymbol{q},\dot{q}) + \boldsymbol{G}(\boldsymbol{q}) = \tau \tag{1}$$

where $\boldsymbol{q} \in \boldsymbol{R}^n$ represents the vector of joint angles, $\boldsymbol{M(q)} \in \boldsymbol{R}^{n \times n}$ denotes the inertial $(n \times n)$ matrix, $\boldsymbol{C}(\boldsymbol{q},\dot{q}) \in \boldsymbol{R}^n$ represents the Coriolis force matrix, $\boldsymbol{G}(\boldsymbol{q}) \in \boldsymbol{R}^n$ denotes the gravitation matrix, and $\tau \in \boldsymbol{R}^n$ represents the joint torque matrix.

A 2-DOF serial PAM robot is used as our simulated robotic manipulator illustrated in Figure 3.

The dynamics of the investigated 2-DOF serial PAM robot is described as follows

$$\boldsymbol{M}(\boldsymbol{q})\ddot{q} + \boldsymbol{C}(\boldsymbol{q},\dot{q}) = \tau \tag{2}$$

where

$$M(q) = \begin{bmatrix} m_1 l^2 + 2m_2 l^2 + 2m_2 l^2 \cos q_2 & m_2 l^2 + m_2 l^2 \cos q_2 \\ m_2 l^2 + m_2 l^2 \cos q_2 & m_2 l^2 \end{bmatrix} = \begin{bmatrix} P_1 + 2P_2 + 2P_2 \cos q_2 & P_1 + P_2 \cos q_2 \\ P_1 + P_2 \cos q_2 & P_2 \end{bmatrix} \tag{3}$$

$$C(q,\dot{q}) = \begin{bmatrix} -2m_2 l^2 \dot{q}_1 \dot{q}_2 \sin q_2 - m_2 l^2 \dot{q}_2^2 \sin q_2 \\ m_2 l^2 \dot{q}_1^2 \sin q_2 \end{bmatrix} = \begin{bmatrix} -2P_2 \dot{q}_1 \dot{q}_2 \sin q_2 - P_2 \dot{q}_2^2 \sin q_2 \\ P_2 \dot{q}_1^2 \sin q_2 \end{bmatrix} \tag{4}$$

Our aim is to control the serial PAM robot (equation (2)) to accurately follow the desired trajectory $\boldsymbol{q}_d$ based on SMC controller. The value of $\dot{q}$ is extracted from $\boldsymbol{C}(\boldsymbol{q},\dot{q})$ (equation (2)) and is rewritten in equation (5) as

$$\tau = \boldsymbol{M}(\boldsymbol{q})\ddot{q} + \boldsymbol{C}_1(\boldsymbol{q},\dot{q})\dot{q} \tag{5}$$

where

$$C_1(q,\dot{q}) = \begin{bmatrix} -P_2 \dot{q}_2 \sin q_2 & -P_2 \dot{q}_1 \sin q_2 - P_2 \dot{q}_2 \sin q_2 \\ P_2 \dot{q}_1 \sin q_2 & 0 \end{bmatrix} \tag{6}$$

The tracking error is defined as

$$\boldsymbol{e} = \boldsymbol{q} - \boldsymbol{q}_d \tag{7}$$

where $\boldsymbol{q} = [q_1, q_2]^{\mathrm{T}}$ and $\boldsymbol{q}_{\mathrm{d}} = [q_{1\mathrm{d}}, q_{2\mathrm{d}}]^{\mathrm{T}}$

Then, the sliding surface is defined as

$$s = \dot{e} + \lambda e \tag{8}$$

where $\lambda = \mathrm{diag}[\lambda_1, \lambda_2]$, in which $\lambda_1$ and $\lambda_2$ are selected as the bandwidth of the 2-DOF serial PAM robot control.

It also needs to select $\tau$ to confirm the sufficient requirement. First the reference state is defined as

$$\dot{q}_r = \dot{q} - s = \dot{q}_d - \lambda e \tag{9}$$

Then the control input $\tau$ is determined as

$$\tau = \hat{M}\ddot{q}_r + \hat{C}_1 \dot{q}_r - \boldsymbol{A}\boldsymbol{s} - \boldsymbol{K}\,\mathrm{sgn}(s) \tag{10}$$

where $\hat{M}$ and $\hat{C}_1$ represent the estimation values of $\boldsymbol{M(q)}$ and $\boldsymbol{C}_1(\boldsymbol{q},\dot{q})$, $\boldsymbol{A} = \mathrm{diag}[a_1, a_2]$, $\dot{q}_r$ represents reference state, sgn($s$) denotes the sign function, and $\boldsymbol{K} = \mathrm{diag}[K_1, K_2]$ represent diagonal positive definite vectors.

Using equations (5) and (10), it gives

$$\boldsymbol{M}\dot{s} + (\boldsymbol{C}_1 + \boldsymbol{A})s = \Delta f - \boldsymbol{K}\,\mathrm{sgn}(s) \tag{11}$$

where $\Delta f = \Delta\hat{M}\ddot{q}_r + \Delta\hat{C}_1\dot{q}_r$, $\Delta\boldsymbol{M} = \hat{M} - \boldsymbol{M}$, and $\Delta\boldsymbol{C}_1 = \hat{C}_1 - \boldsymbol{C}_1$. It assumes that the bound $|\Delta f_i|_{\mathrm{bound}}$ of $\Delta fi\,(i = 1, 2)$ is determined. Thus, the value $\boldsymbol{K}$ is chosen as

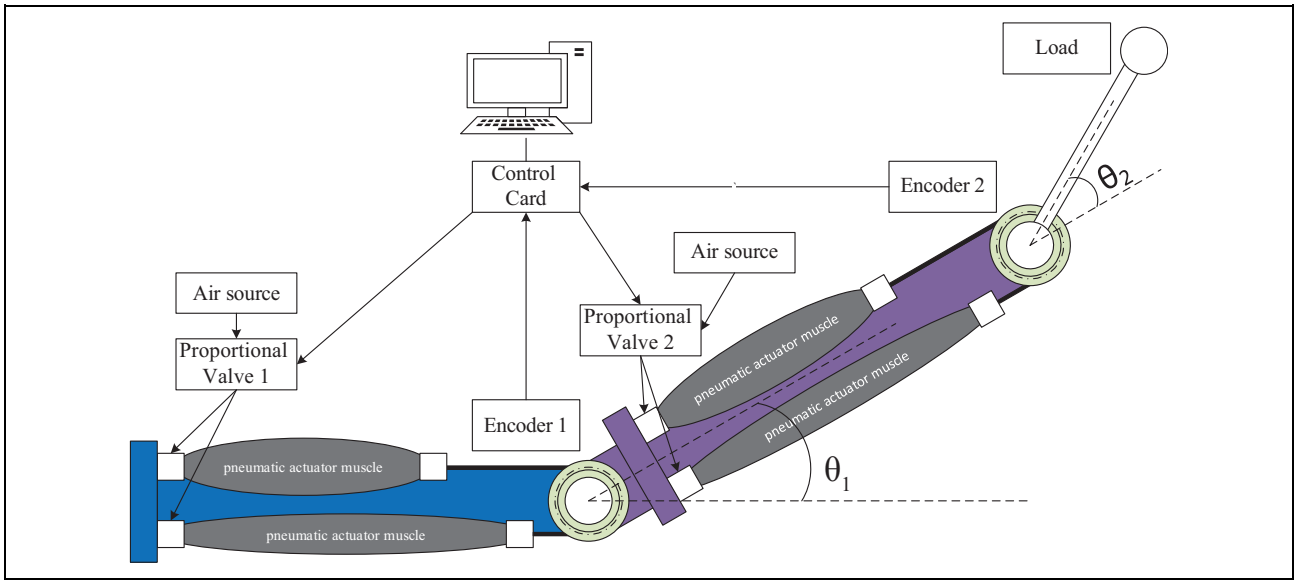


**Figure 2.** Experimental configuration of the 2-DOF serial PAM robot. DOF: degrees of freedom; PAM: pneumatic artificial muscle manipulator.

**Table 1.** Lists of the experimental configuration setup

| No. | Name | Model name | Company |
|---|---|---|---|
| 1 | Proportional valve (2) | MPYE-5-1/8HF-710 B | FESTO (Germany) |
| 2 | Pneumatic artificial muscle (4) | MAS-10-N-220-AA-MCFK | FESTO (Germany) |
| 3 | D/A board | PCI 1720 | ADVANTECH (Taiwan) |
| 4 | Counter board | PCI QUAD-4 | COMPUTING MEASUREMENT (USA) |
| 5 | Rotary encoder (2) | H40-8-3600Z0 | METRONIX (South Korea) |

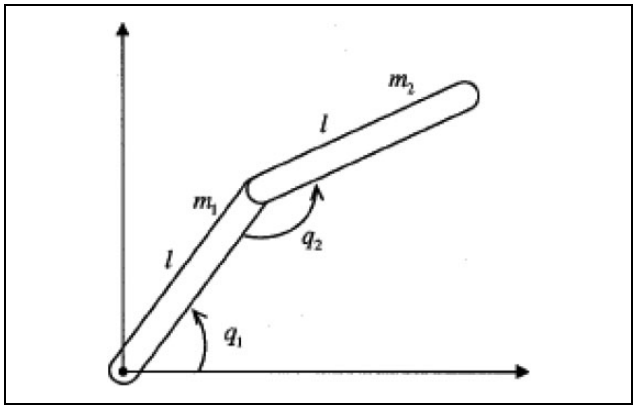


**Figure 3.** Compact structure of the 2-DOF serial PAM robot. DOF: degrees of freedom; PAM: pneumatic artificial muscle manipulator.

$$K_i \geq |\Delta f_i|_{\text{bound}} \tag{12}$$

Then the Lyapunov function candidate is described as

$$V = \frac{1}{2} s^T M s \tag{13}$$

Since $\boldsymbol{M}$ is positive symmetric definite, we have $V > 0$ with $s \neq 0$. The derivative of $\boldsymbol{M}$ with respect to time in equation (3) now is calculated as

$$\dot{M} = \begin{bmatrix} -2m_2 l^2 \dot{q}_2 \sin q_2 & -m_2 l^2 \dot{q}_2 \sin q_2 \\ -m_2 l^2 \dot{q}_2 \sin q_2 & 0 \end{bmatrix} \tag{14}$$

From equations (11) and (14), it gives

$$\dot{M} - 2C_1 = \begin{bmatrix} 0 & 2m_2 l^2 \dot{q}_1 \sin q_2 + m_2 l^2 \dot{q}_2 \sin q_2 \\ -2m_2 l^2 \dot{q}_1 \sin q_2 - m_2 l^2 \dot{q}_2 \sin q_2 & 0 \end{bmatrix} \tag{15}$$

which represents a skew-symmetric matrix satisfying

$$s^T (\dot{M} - 2C_1) s = 0 \tag{16}$$

Then $\dot{V}$ can be calculated as

$$\begin{aligned} \dot{V} &= s^T M \dot{s} + \frac{1}{2} s^T \dot{M} s \\ &= s^T (M \dot{s} + \boldsymbol{C}_1 s) \\ &= s^T [-As + \Delta f - K \operatorname{sgn}(s)] \\ &= \sum_{i=1}^{2} (s_i [\Delta f_i - K_i \operatorname{sgn}(s_i)] - s^T A s) \end{aligned} \tag{17}$$

For $K_i \geq |\Delta f_i|$, we always get $s_i[\Delta f_i - K_i \operatorname{sgn}(s_i)] \leq 0$. Then $\dot{V}$ is described as

$$\dot{V} = \sum_{i=1}^{2} \left( s_i[\Delta f_i - K_i \operatorname{sgn}(s_i)] \right) - s^T A s \leq -s^T A s < 0 \quad (s \neq 0) \tag{18}$$

To remove the chattering issue, a saturation function is applied in the control rule instead of the sign function as presented in equation (10). The control rule has the form as,

$$\tau = \hat{M}\ddot{q}_r + \hat{C}_1 \dot{q}_r - As - K\text{sat}(s/\Phi) \tag{19}$$

In this standard SMC approach, the model of the serial PAM robot is partly undetermined. It needs to know the model structure of the serial PAM robot. But we can't determine the exact values of $m_1 l^2$ and $m_2 l^2$ in $\boldsymbol{M}$ and $\boldsymbol{C}_1$. We define $p_1 = m_1 l^2$ and $p_2 = m_2 l^2$. We also define $\hat{p}_1$ and $\hat{p}_2$ representing the estimated values of $p_1$ and $p_2$. If the values of $\hat{p}_1$ and $\hat{p}_2$ are far away from the real values, it needs to increase the control gain $\boldsymbol{K}$ to prevent the tracking error in equation (7) getting worse. The chattering problem may be eliminated by using the saturation function in equation (19). Unfortunately, there is no theoretical Lyapunov stability proof for this control rule presented in equation (19).

We simulate this classic SMC method for the 2-DOF serial PAM robot. We pick $p_1 = 1$ and $p_2 = 2$. Since serial PAM robot cannot instantaneously follow a step sequence, the desired trajectory will be the output of the filtered sequential values of unit steps. We define the transfer function of prefilter for each joint of the serial PAM robot as

$$W_m(s) = \frac{2}{s^2 + 4s + 4} \tag{20}$$

The beginning values of the serial PAM robot's joint positions are set to 0.5 rad. The estimated dynamics of the serial PAM robot are $\hat{p}_1 = 1.5$ and $\hat{p}_2 = 3$. We pick $\lambda$ in equation (8) as the same bandwidth as in equation (20). It first simply picks $\boldsymbol{A} = \text{diag}[1, 1]$ in equation (10). To decide $\boldsymbol{K}$ in equation (10), it is necessary to determine the real $\Delta f$ value presented in equation (18).

First we choose $\boldsymbol{K} = [20, 10]^{\text{T}}$. We run simulation and plot $\Delta f$. Then we get $|\Delta f|_1 \leq 45$ and $|\Delta f_2| \leq 21$. This will fail the criterion in equation (12). To satisfy this criterion, we choose $\boldsymbol{K} = [45, 21]^{\text{T}}$ and simulate again.

Figure 4 represents the tracking performance and the tracking error of the 1st joint of serial PAM robot in classic SMC. Figure 5 describes the results of control input value and the SMC surface of the 1st joint of serial PAM robot in SMC. Similarly, Figure 6 presents the tracking performance and the tracking error of the 2nd joint of serial PAM robot in classic SMC. Figure 7 illustrates the results of control input value and the SMC surface of the 2nd joint of the serial PAM robot in SMC. Figures 4 and 6 show that the tracking accuracy is obtained with significant error. The drawback rests here related to the chattering problem significantly exists as shown in Figures 5 and 7.

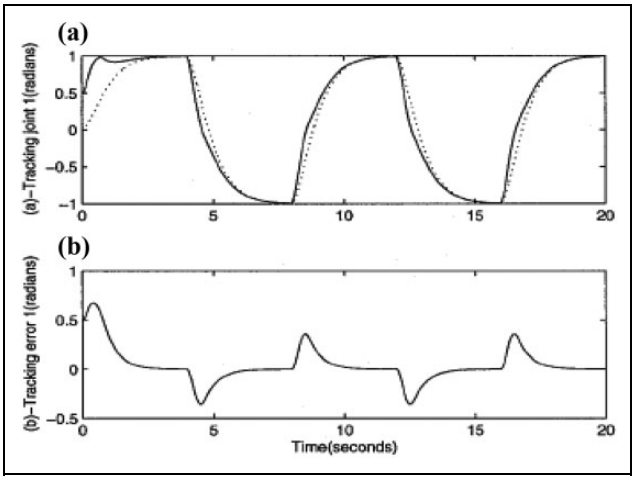


**Figure 4.** (a) Tracking and (b) errors of the 1st joint of serial PAM robot in classic SMC. Dash line: desired trajectory; solid line: actual trajectory; PAM: pneumatic artificial muscle manipulator; SMC: sliding mode control.

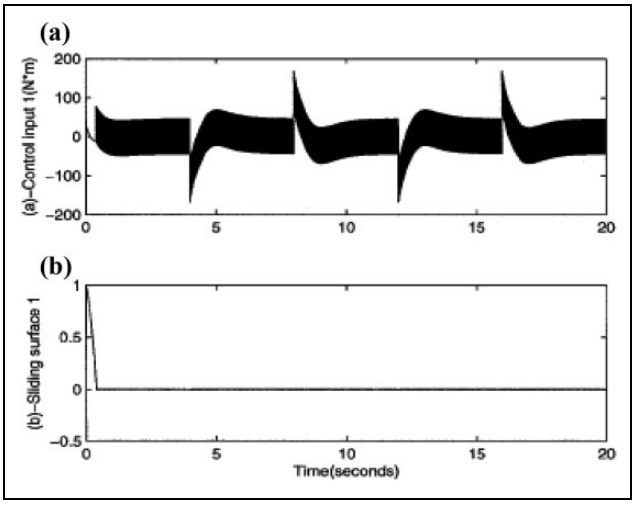


**Figure 5.** (a) Control input value and (b) SMC surface of the 1st joint of serial PAM robot in classic SMC. SMC: sliding mode control; PAM: pneumatic artificial muscle manipulator.

From the above results, it is clear to notice that SMC can deal with nonlinear systems especially for the nonlinear and uncertain serial PAM robot. The control input forces the serial PAM robot to track the desired trajectories. The drawback related to the chattering issue is attenuated based on the saturation function applied in the control rule. The Lyapunov stability theorem is proved only in the case of the sign function applied in the control rule. Thus the classical SMC can be used to control the serial PAM robot under the condition of partly known model dynamics. In the next section, the proposed EAFSMC system is initiatively applied to successfully estimate and robustly control the serial PAM robot systems.

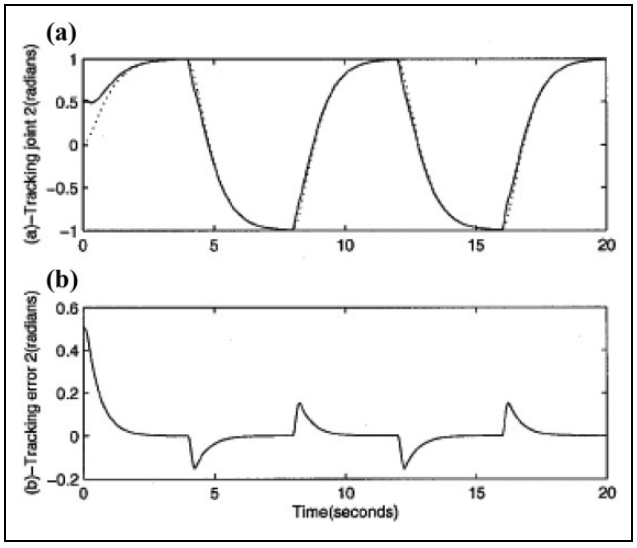


**Figure 6.** (a) Tracking and (b) errors of the 2nd joint of serial PAM robot in classic SMC. Dash line: desired trajectory; solid line: actual trajectory; PAM: pneumatic artificial muscle manipulator; SMC: serial mode control.

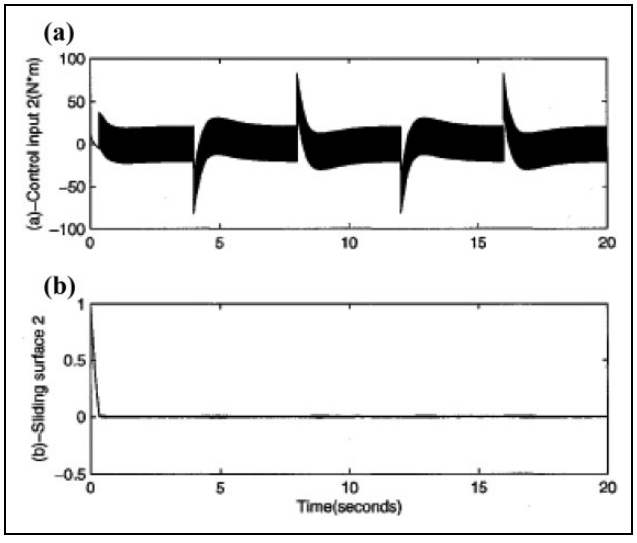


**Figure 7.** (a) Control input value and (b) SMC surface of the 2nd joint of serial PAM robot in classic SMC. SMC: sliding mode control; PAM: pneumatic artificial muscle manipulator.

## Proposed EAFSMC

The previous results show that the traditional SMC controller encounters difficulty in controlling unstructured system uncertainties. In order to solve this task, this article proposes novel EAFSMC algorithm by combining SMC and specific fuzzy model. The new concept here relies on the fact that the addition of an adaptation law to a FSMC helps ameliorate the system's tracking performance via online updating the parameters of the fuzzy rules. Then, the new EAFSMC algorithm applied to position control of a two-link serial PAM robot is introduced in detail.

In general, the dynamic equation of an $m$-link serial PAM robot is described as

$$\boldsymbol{M}(\boldsymbol{q})\ddot{q} + \boldsymbol{C}(\boldsymbol{q},\dot{q}) + \boldsymbol{G}(\boldsymbol{q}) = \tau \tag{21}$$

where $\boldsymbol{q} = [q_1, \ldots, q_m]^{\mathrm{T}}$ represents an $m \times 1$ vector of joint position, $\boldsymbol{M}(\boldsymbol{q})$ represents an $m \times m$ inertial vector matrix, $\boldsymbol{C}(\boldsymbol{q},\dot{q})$ denotes an $m \times 1$ matrix of Coriolis torques, $\boldsymbol{G(q)}$ denotes an $m \times 1$ gravity matrix, and $\tau = [\tau_1, \ldots\ldots\ldots, \tau_m]^{\mathrm{T}}$ denotes an $m \times 1$ vector of joint torques.

### Proposed EAFSMC algorithm implementation

This article introduces a novel EAFSMC algorithm applied to improve the tracking control performance of the 2-DOF serial PAM robot. The new fuzzy model used in this method is a multiple inputs multiple outputs fuzzy system whose fuzzy if-then laws are perfectly reduced by considering the SMC surfaces as the input variable.

We rewrite equation (21) as

$$\begin{aligned}\ddot{q} &= -M^{-1}(q)\,C(q,\dot{q}) - M^{-1}(q)\,G(q) + M^{-1}(q)\tau \\ &= F(q,\dot{q}) + B(q)\tau\end{aligned} \tag{22}$$

where $\boldsymbol{F}(\boldsymbol{q},\dot{q}) = -\boldsymbol{M}^{-1}(\boldsymbol{q})\,\boldsymbol{C}(\boldsymbol{q},\dot{q}) - \boldsymbol{M}^{-1}(\boldsymbol{q})\,\boldsymbol{G}(\boldsymbol{q})$ and $\boldsymbol{B}(\boldsymbol{q}) = \boldsymbol{M}^{-1}(\boldsymbol{q})$.

Then, the sliding surface is defined as

$$s = \dot{e} + \lambda e \tag{23}$$

where $\boldsymbol{e} = \boldsymbol{q} - \boldsymbol{q}_d$. We take the derivative of $\boldsymbol{s}$ and get

$$\dot{s} = \ddot{e} + \lambda\dot{e} = \boldsymbol{F}(\boldsymbol{q},\dot{q}) + \boldsymbol{B}(\boldsymbol{q})\tau - \ddot{q}_d + \lambda\dot{e} \tag{24}$$

Let $\dot{s} = 0$ in equation (24) and then derive the ideal SMC law $\tau^*$

$$\tau^* = \boldsymbol{B}(\boldsymbol{q})^{-1}[\ddot{q}_d - \boldsymbol{F}(\boldsymbol{q},\dot{q}) - \lambda\dot{e} - K_M\,\mathrm{sgn}(s)] \tag{25}$$

where $\boldsymbol{K}_M = \mathrm{diag}[K_{\mathrm{M1}}, \ldots, K_{\mathrm{Mm}}]$ and $K_{\mathrm{M1}}, \ldots, K_{\mathrm{Mm}}$ represent positive constants. The control law is defined as

$$\tau = \hat{B}^{-1}(s|\theta_B)(\ddot{q}_d - \hat{F}(s|\theta_F) - \lambda\dot{e} - \hat{H}(s|\theta_H)) \tag{26}$$

in which $\hat{F}(s|\theta_F)$, $\hat{B}(s|\theta_B)$, and $\hat{H}(s|\theta_H)$ represent fuzzy systems designed to estimate $\boldsymbol{F}(\boldsymbol{q},\dot{q})$, $\boldsymbol{B}(\boldsymbol{q})$ and $\boldsymbol{K}_M\mathrm{sgn}(\boldsymbol{s})$ in equation (25). The fuzzy model $\hat{F}(s|\theta_F)$ is implemented by $\hat{F}(s|\theta_F) = [\hat{f}_1(s|\theta_{f_1}), \ldots\ldots, \hat{f}_m(s|\theta_{f_m})]^{\mathrm{T}}$ with

$$\hat{f}_j(s|\theta_{f_j}) = \frac{\sum_{l=1}^{M}\theta_{f_i}^{l}\left(\prod_{i=1}^{m}\mu A_i^l(s_i)\right)}{\sum_{l=1}^{M}\left(\prod_{i=1}^{m}\mu A_i^l(s_i)\right)} = \theta_{f_i}^{T}\xi(s) \tag{27}$$

The fuzzy system $\hat{B}(s|\theta_B)$ is defined as

$$\hat{B}(s|\theta_B) = \begin{bmatrix} \hat{b}_{11}(s|\theta_{b11}), & \ldots & \hat{b}_{1m}(s|\theta_{b1m}), \\ \ldots & \ldots & \ldots \\ \hat{b}_{m1}(s|\theta_{bm1}), & \ldots & \hat{b}_{mm}(s|\theta_{bmm}), \end{bmatrix} \tag{28}$$

where

$$\hat{b}_{jk}(s|\theta_{f_j}) = \frac{\sum_{l=1}^{M} \theta_{b_{jk}}^{l} (\prod_{i=1}^{m} \mu_{A_i^l}(s_i))}{\sum_{l=1}^{M} (\prod_{i=1}^{m} \mu_{A_i^l}(s_i))} = \theta_{b_{jk}}^{T} \xi(s) \tag{29}$$

The novel fuzzy model $\hat{H}(s|\theta_H)$ is designed as $\hat{H}(s|\theta_H) = [\hat{h}_1(s_1|\theta_{h_1}), ..., \hat{h}_m(s_m|\theta_{h_m})]^T$ with

$$\hat{h}_j(s_j|\theta_{f_j}) = \frac{\sum_{l=1}^{M} \theta_{h_j}^{l} \mu_{A_i^l}(s_j)}{\sum_{l=1}^{M} \mu_{A_i^l}(s_j)} = \theta_{h_j}^{T} \xi(s_j) \tag{30}$$

Then the adaptation laws are described as

$$\begin{aligned} \dot{\theta}_{fj} &= -\chi_{fj}\, s_j\, \xi(s) \\ \dot{\theta}_{bjk} &= -\chi_{bjk}\, s_j\, \xi(s) \\ \dot{\theta}_{hj} &= -\chi_{hj}\, s_j\, \xi(s_j) \end{aligned} \tag{31}$$

where $\chi_{f_j}$, $\chi_{b_{jk}}$, and $\chi_{h_j}$ denote constantly positive values.

### *Stability proof of the proposed EAFSMC algorithm*

First, it needs to define the minimum approximation errors as

$$\omega_F = F(q, \dot{q}) - \hat{F}(s|\theta_F^*) = [\omega_{f_1}, ..., \omega_{fm}]^T \tag{32}$$

$$\omega_B = B(q) - \hat{B}(s|\theta_B^*),\ \omega_{b_{jk}} = b_{jk}(q) - \hat{b}_{jk}(s|\theta_{b_{jk}}) \tag{33}$$

$$\omega_H = K_M\, \mathrm{sgn}(s) - \hat{H}(s|\theta_H^*) = [\omega_{h_1}, ..., \omega_{hm}]^T \tag{34}$$

where $\boldsymbol{K}_M = \mathrm{diag}[K_{\mathrm{M1}}, \ldots, K_{\mathrm{Mm}}]$ and $K_{\mathrm{M1}}, \ldots, K_{\mathrm{Mm}}$ are positive constants. From equation (26), we get

$$\ddot{q}_d = \hat{B}(s|\theta_B)\tau + \hat{F}(s|\theta_F) + \lambda\dot{e} + \hat{H}(s|\theta_H) \tag{35}$$

Put (equation (35)) into (equation (24)), it leads to

$$\begin{aligned} \dot{s} &= F(q,\dot{q}) + B(q)\tau - \left(\dot{\hat{B}}(s|\theta_B)\tau + \dot{\hat{F}}(s|\theta_B) + \lambda\dot{e} + H(s|\theta_H)\right) + \lambda\dot{e} \\ &= F(q,\dot{q}) - \hat{F}(s|\theta_F) + \left(B(q) - \hat{B}(s|\theta_B)\right)\tau - \hat{H}(s|\theta_H) \\ &= \hat{F}(s|\theta_F^*) - \hat{F}(s|\theta_B) + \omega_F + \left(\hat{B}(s|\theta_B^*) - \hat{B}(s|\theta_B) + \omega_B\right)\tau \\ &\quad + \hat{H}(s|\theta_H^*) - \hat{H}(s|\theta_H) - \hat{H}(s|\theta_H^*) \end{aligned} \tag{36}$$

Then for each $s_j$, we can rewrite as

$$\begin{aligned} \dot{s}_j &= \dot{\hat{f}}_j(s|\theta_{f_j}^*) - \dot{\hat{f}}_j(s|\theta_{f_j}) + \omega_{f_j} + \sum_{k=1}^{m}\left(\hat{b}_{jk}(s|\theta_{b_{jk}}^*) - \hat{b}_{jk}(s|\theta_{b_{jk}}) + \omega_{b_{jk}}\right)\tau_j \\ &\quad + \dot{\hat{h}}_j(s_j|\theta_{h_j}^*) - \dot{\hat{h}}_j(s_j|\theta_{h_j}) - \dot{\hat{h}}_j(s_j|\theta_{h_j}^*) \\ &= \phi_{f_j}^T \xi(s) + \omega_{f_j} + \sum_{k=1}^{m}\left(\phi_{b_{jk}}^T \xi(s) + \omega_{b_{jk}}\right)\tau_j + \phi_{h_j}^T \xi(s) - \dot{\hat{h}}_j(s_j|\theta_{h_j}^*) \end{aligned} \tag{37}$$

where $\phi_{f_j} = \theta_{f_j}^* - \theta_{f_j}$, $\phi_{b_{jk}} = \theta_{b_{jk}}^* - \theta_{b_{jk}}$, and $\phi_{h_j} = \theta_{h_j}^* - \theta_{h_j}$.

The followed Lyapunov function $V_j$ is defined for each joint of the serial PAM robot

$$V_j = \frac{1}{2}\left(s_j^2 + \frac{1}{\chi_{f_j}}\phi_{f_j}^T\phi_{f_j} + \sum_{k=1}^{m}\frac{1}{\chi_{b_{jk}}}\phi_{b_{jk}}^T\phi_{b_{jk}} + \frac{1}{\chi_{h_j}}\phi_{h_j}^T\phi_{h_j}\right) \tag{38}$$

The derivative of $V_j$ is determined as

$$\begin{aligned} \dot{V}_j &= s_j\dot{s}_j + \frac{1}{\chi_{f_j}}\phi_{f_j}^T\dot{\phi}_{f_j} + \sum_{k=1}^{m}\frac{1}{\chi_{b_{jk}}}\phi_{b_{jk}}^T\dot{\phi}_{b_{jk}} + \frac{1}{\chi_{h_j}}\phi_{h_j}^T\dot{\phi}_{h_j} \\ &= s_j\left(\phi_{f_j}^T\xi(s) + \sum_{k=1}^{m}\phi_{b_{jk}}^T\xi(s) + \phi_{h_j}^T\xi(s_j)\right) + \frac{1}{\chi_{f_j}}\phi_{f_j}^T\dot{\phi}_{f_j} + \sum_{k=1}^{m}\frac{1}{\chi_{b_{jk}}}\phi_{b_{jk}}^T\dot{\phi}_{b_{jk}} \\ &\quad + \frac{1}{\chi_{h_j}}\phi_{h_j}^T\dot{\phi}_{h_j} + s_j\left(\omega_{f_j} + \sum_{k=1}^{m}\omega_{b_{jk}}\tau_j\right) - s_j\dot{\hat{h}}_j(s_j|\theta_{h_j}^*) \\ &= \frac{1}{\chi_{f_j}}\phi_{f_j}^T\left(\chi_{f_j}s_j\xi(s) + \dot{\phi}_{f_j}\right) + \sum_{k=1}^{m}\frac{1}{\chi_{b_{jk}}}\phi_{b_{jk}}^T\left(\chi_{b_{jk}}s_j\xi(s) + \dot{\phi}_{b_{jk}}\right) \\ &\quad + \frac{1}{\chi_{h_j}}\phi_{h_j}^T\left(\chi_{h_j}s_j\xi(s_j) + \dot{\phi}_{h_j}\right) + s_j(\omega_{f_j} + \sum_{k=1}^{m}\omega_{b_{jk}}\tau_j + \omega_{h_j}) - s_jK_{M_j}\,\mathrm{sgn}(s_j) \\ &= \frac{1}{\chi_{f_j}}\phi_{f_j}^T\left(\chi_{f_j}s_j\xi(s) + \dot{\phi}_{f_j}\right) + \sum_{k=1}^{m}\frac{1}{\chi_{b_{jk}}}\phi_{b_{jk}}^T\left(\chi_{b_{jk}}s_j\xi(s) + \dot{\phi}_{b_{jk}}\right) \\ &\quad + \frac{1}{\chi_{h_j}}\phi_{h_j}^T\left(\chi_{h_j}s_j\xi(s_j) + \dot{\phi}_{h_j}\right) + s_j\Omega_j - K_{M_j}|s_j| \end{aligned} \tag{39}$$

where $\Omega_j = \omega_{fj} + \sum_{k=1}^{m}\omega_{b_{jk}}\tau_j + \omega_{h_j}$. The adaptation laws are given in equation (31). Then we can rewrite equation (39) as

$$\dot{V}_j = s_j\Omega_j - K_{Mj}|s_j| \le (|\Omega_j| - K_{Mj})|s_j| \tag{40}$$

According to Universal Approximation Theorem, $\Omega_j$ proves as small as possible. Therefore, it is simple to pick $\boldsymbol{K}_{mj} > |\Omega_j|$ and get $\dot{V}_j < 0$ for $s \neq 0$.

In summary, the novel EAFSMC algorithm is proposed with the adaptation laws designed with respect to the Lyapunov stability theorem. The convergence and stability of the closed-loop serial PAM robot is mathematically demonstrated based on the Lyapunov stability principle.

## Simulation results

### *Dynamic equations of the 2-joint serial PAM robot*

The dynamic equations for the 2-joint serial PAM robot are calculated as

$$\tau = \boldsymbol{M}(\boldsymbol{q})\ddot{q} + \boldsymbol{C}(\boldsymbol{q},\dot{q}) = \boldsymbol{M}(\boldsymbol{q})\ddot{q} + \boldsymbol{C}_1(\boldsymbol{q},\dot{q})\dot{q} \tag{41}$$

$$M(q) = \begin{bmatrix} m_1 l^2 + 2m_2 l^2 + 2m_2 l^2 \cos q_2 & m_2 l^2 + m_2 l^2 \cos q_2 \\ m_2 l^2 + m_2 l^2 \cos q_2 & m_2 l^2 \end{bmatrix} = \begin{bmatrix} P_1 + 2P_2 + 2P_2 \cos q_2 & P_1 + P_2 \cos q_2 \\ P_1 + P_2 \cos q_2 & P_2 \end{bmatrix} \tag{42}$$

$$C(q,\dot{q}) = \begin{bmatrix} -2m_2 l^2 \dot{q}_1 \dot{q}_2 \sin q_2 - m_2 l^2 \dot{q}_2^2 \sin q_2 \\ m_2 l^2 \dot{q}_1^2 \sin q_2 \end{bmatrix} = \begin{bmatrix} -2P_2 \dot{q}_1 \dot{q}_2 \sin q_2 - P_2 \dot{q}_2^2 \sin q_2 \\ P_2 \dot{q}_1^2 \sin q_2 \end{bmatrix} \tag{43}$$

$$C_1(q,\dot{q}) = \begin{bmatrix} -P_2 \dot{q}_2 \sin q_2 & -P_2 \dot{q}_1 \sin q_2 - P_2 \dot{q}_2 \sin q_2 \\ P_2 \dot{q}_1 \sin q_2 & 0 \end{bmatrix} \tag{44}$$

where $m_1$, $m_2$ represent the mass of links 1 and 2, respectively; $l$ denotes the length of links 1 and 2; and $q_1$ and $q_2$ represent the joint-angle positions of links 1 and 2, respectively. The values of the parameters are chosen as $P_1 = m_1 l^2 = 1$ and $P_2 = m_2 l^2 = 2$. The serial PAM robot model's transfer function for each link is described as

$$W_m(s) = \frac{4}{s^2 + 4s + 4} \tag{45}$$

The required trajectory is the output of filtered sequential unique steps. The starting values of the serial PAM robot's joint-angle positions are given as 0.5 rad. Throughout the proposed algorithm, we choose the parameter $\lambda_j$ in the sliding surface as same as the bandwidth of the desired model. The predefined adaptation gains in adaptation laws are selected as a *trial* and *error values*.

## Control results of the proposed EAFSMC method

The novel EAFSMC approach is able to adaptively estimate online the dynamic features of the 2-DOF serial PAM robot presented in equation (41). Then, the proposed EAFSMC algorithm is quite available for controlling the nonlinear serial PAM robot system containing uncertain dynamic characteristics. The advantage of EAFSMC algorithm is to successfully and robustly remove the chattering issue using the new fuzzy-based compensators in the control rule. In comparison with FSMC algorithm applied in the serial PAM robot,[22] the number of new fuzzy if-then laws is significantly reduced by applying the SMC surfaces as the inputs with the proposed EAFSMC method.

Concretely we select $k_1 = 5$, $k_2 = 7$ as the number of fuzzy membership functions (MPs) for each input value, namely NM NS ZO PS PM and NB NM NS ZO PS PM PB, respectively. The parameters of the fuzzy MPs for $s_j$ are selected using the simulation results of the sliding surface $s_j$ realized in the "SMC of the 2-DOF Serial PAM robot" section. The membership functions for the variable $s_j$ ($j = 1, 2$), described in Figure 8, are expressed as

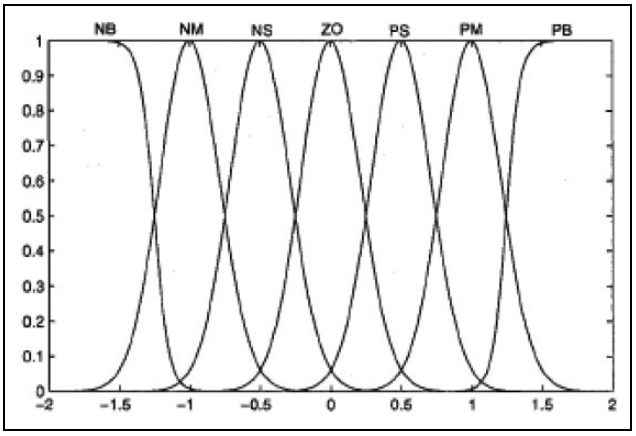


**Figure 8.** Membership functions of $s_j$.

$$\begin{aligned}
\mu_{s_j NB} &= \frac{1}{1 + [\exp\Big((s_j + 1.25)/0.1\Big)]^2} \\
\mu_{s_j NM} &= \exp\Big( - \Big((s_j + 1)/0.3\Big)^2\Big) \\
\mu_{s_j NS} &= \exp\Big( - \Big((s_j + 0.5)/0.3\Big)^2\Big) \\
\mu_{s_j ZO} &= \exp\Big( - (s_j/0.3)^2\Big) \\
\mu_{s_j PS} &= \exp\Big( - \Big((s_j - 0.5)/0.3\Big)^2\Big) \\
\mu_{s_j PM} &= \exp\Big( - \Big((s_j - 1)/0.3\Big)^2\Big) \\
\mu_{s_j PB} &= \frac{1}{1 + [\exp\Big( - (s_j - 1.25)/0.1\Big)]^2}
\end{aligned} \tag{46}$$

The structure of MPs for each input is defined as in equation (46). Since there is an inverse matrix $\hat{B}^{-1}(s|\theta_B)$ in the control law (equation (26)), we have to define an initial condition for the proposed fuzzy model $\hat{B}(s|\theta_B)$. The initial value of $\hat{B}\Big(s(0)|\theta_B(0)\Big)$ is chosen as $\hat{B}\Big(s(0)|\theta_B(0)\Big) = \text{diag}[1, 2]$. The parameters of the adaptive fuzzy rules described in equation (31) are determined as $\chi_{f_j} = 4.5 \times 10^3$ ($j = 1, 2$), $\chi_{b_{jk}} = 4.5 \times 10^3$ ($j, k = 1, 2$), and $\chi_{h_j} = 0.02$ ($j = 1, 2$).

Figure 9 represents the tracking performance and the tracking error of the 1st joint of the serial PAM robot with proposed EAFSMC. Figure 10 describes the results of control input value and the SMC surface of the 1st joint of the serial PAM robot with proposed EAFSMC. Continually, Figure 11 presents the tracking performance and the tracking error of the 2nd joint of the serial PAM robot with proposed EAFSMC. Finally, Figure 12

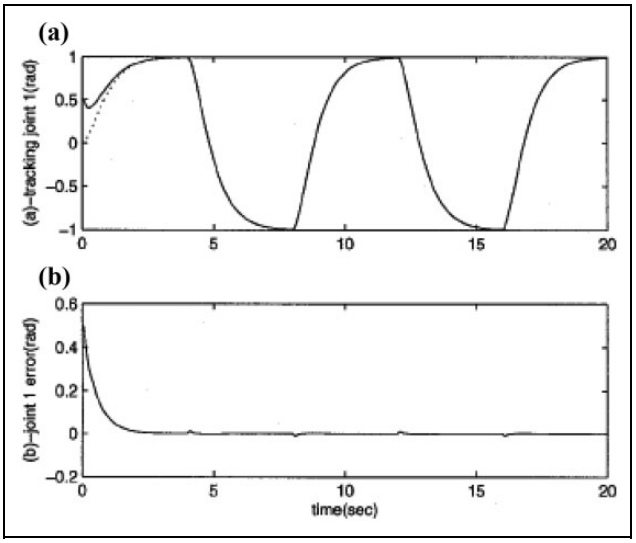


**Figure 9.** (a) Joint-angle tracking performance and (b) joint-angle tracking errors of joint 1 of serial PAM robot with proposed advanced EAFSMC algorithm. Dash line: required trajectory; solid line: real trajectory. PAM: pneumatic artificial muscle manipulator; EAFSMC: enhanced adaptive fuzzy sliding mode control.

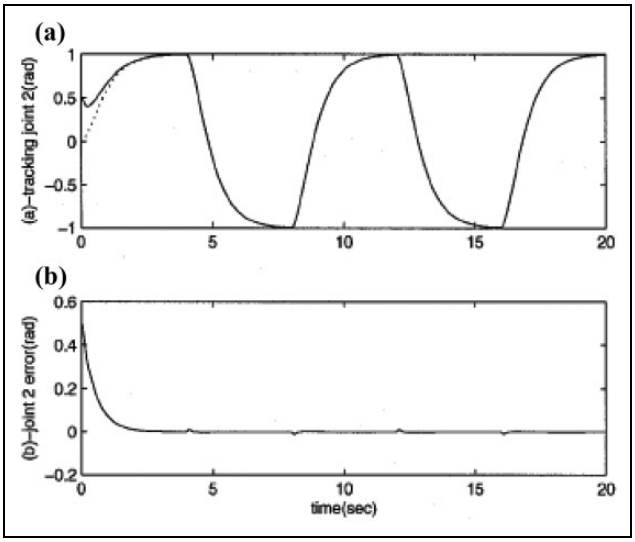


**Figure 11.** (a) Joint-angle tracking performance and (b) joint-angle tracking errors of joint 2 of serial PAM robot with proposed EAFSMC algorithm. Dash line: required trajectory; solid line: real trajectory. PAM: pneumatic artificial muscle manipulator; EAFSMC: enhanced adaptive fuzzy sliding mode control.

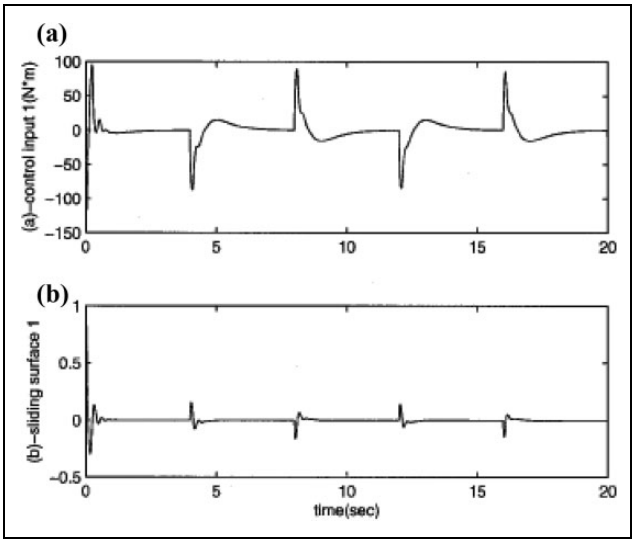


**Figure 10.** (a) Control signal and (b) SMC surface of joint 1 of serial PAM robot with proposed advanced EAFSMC algorithm. SMC: sliding mode control; PAM: pneumatic artificial muscle manipulator; EAFSMC: enhanced adaptive fuzzy sliding mode control.

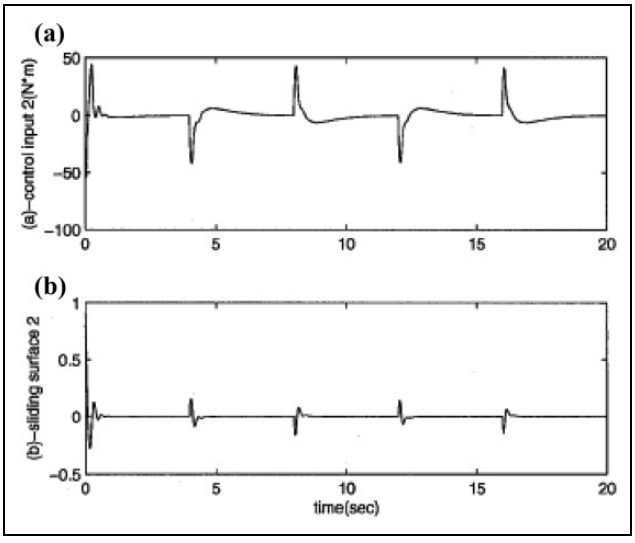


**Figure 12.** (a) Control signal and (b) SMC surface of joint 2 of serial PAM robot with proposed EAFSMC algorithm. SMC: sliding mode control; PAM: pneumatic artificial muscle manipulator; EAFSMC: enhanced adaptive fuzzy sliding mode control.

illustrates the shape of control input value and the SMC surface of the 2nd joint of the serial PAM robot with proposed EAFSMC.

Figures 9 and 11 show that the joint-angle tracking errors are successfully bounded in the limit [−0.005, 0.005] rad. Furthermore, from Figures 10 and 12, it is evident to confirm that the chattering issue is successfully removed by applying the new fuzzy model as an adaptive compensator in the control rule.

Figure 13 presents the comparative ellipsoid trajectory tracking performance of the serial PAM robot system. From this figure, it is evident to see that the proposed EAFSMC method provides more accurate and much better performance than the FSMC applied in the study by Chang[27] and the standard SMC, respectively.

In summary, this article proposes an EAFSMC algorithm to improve the tracking control performance of a highly uncertain nonlinear serial PAM robot. In this

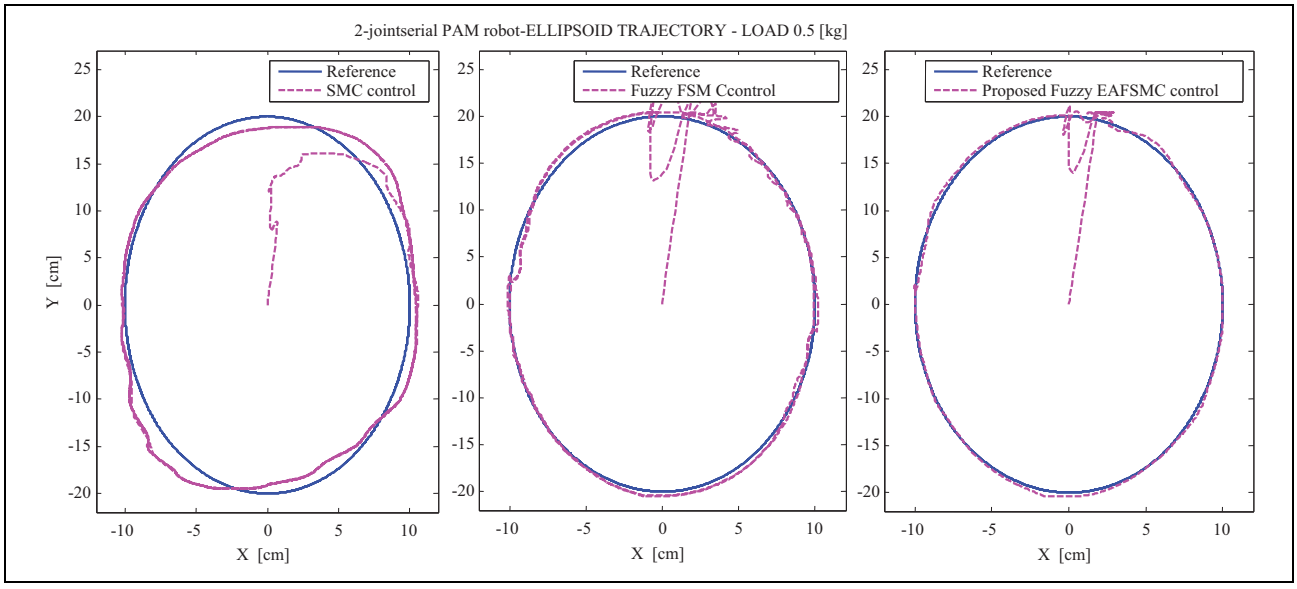


**Figure 13.** Comparative ellipsoid trajectory tracking performance.

**Table 2.** Comparative performance results.

| Algorithms | Availability of tuning method | Number of fuzzy rules | Chattering remove effect | Time-consuming cost | Tracking precision performance |
|---|---|---|---|---|---|
| Adaptive FSMC[27] | Consequence part | $m \times k_2^{2m}$ | Attenuated | High | Mean |
| Hybrid fuzzy CMAC-SMC[28] | Consequence part | $m \times k_2^{2m}$ | Attenuated | High | Mean |
| Proposed EAFSMC | Premise and consequence part | $(m+1) \times k_2^m + k_2$ | Strongly attenuated | Medium | High |

SMC: sliding mode control; CMAC: cerebellar model articulation controller; EAFSMC: enhanced adaptive fuzzy sliding mode control.

approach, the proposed EAFSMC fuzzy system is implemented to adaptively identify the dynamic features of the serial PAM robot. Related to the $m$-DOF serial PAM robot, with $k_2$ MPs designed for each input, the total number of fuzzy *if-then* laws for each joint of the serial PAM robot is $(m+1) \times k_2^m + k_2$. Compared to FSMC algorithms applied by Chang[27] and Shi and Shen,[28] with the number of fuzzy *if-then* rules for each joint of the serial PAM robot is $m \times k_2^{2m}$, it is evident to see that the number of the fuzzy *if-then* laws of the proposed EAFSMC is significantly reduced by implementing SMC surfaces as the inputs of the proposed fuzzy model.

Moreover, comparative results of the novel proposed EAFSMC controller and of FSMC approaches used by Chang[27] and Shi and Shen,[28] applied to the highly nonlinear serial PAM robot system, related to the tracking precision performance, the total time-consuming computation criteria, and so on, are tabulated in Table 2.

Comparative results in Table 2 once more demonstrate better performance of the proposed advanced EAFSMC in comparison with the FSMC by Chang[27] and/or the hybrid fuzzy CMAC-SMC used by Shi and Shen.[28]

## Conclusions

In this article, a novel EAFSMC algorithm is introduced and applied to a 2-DOF serial PAM robot system. The proposed adaptive fuzzy EAFSMC algorithm introduces a new indirect adaptive fuzzy EAFSMC algorithm which successfully identifies the dynamic and cross-coupled features of the serial PAM robot. The convergence and the stability of the proposed EAFSMC method for the 2-DOF serial PAM robot have also been successfully demonstrated based on the Lyapunov stability principle. The comparative results clearly demonstrate the effectiveness of the obtained results, in particular, compared with existing works in the literature.

### Declaration of conflicting interests

The author(s) declared no potential conflicts of interest with respect to the research, authorship, and/or publication of this article.

### Funding

The author(s) disclosed receipt of the following financial support for the research, authorship, and/or publication of this article: This

research was fully funded by Vietnam National University HoChiMinh City (VNU-HCM) under grant number C2018-20-07.

## References


1. Song Q and Chao J. Robust speed controller design for permanent magnet synchronous motor drives based on sliding mode control. *Energ Procedia* 2016; 88: 867–873.
2. Esmaeili N, Alfi A and Khosravi H. Balancing and trajectory tracking of two-wheeled mobile robot using backstepping sliding mode control: design and experiments. *J Intell Robot Syst* 2017; 87(3–4): 601–613.
3. Yang JM and Kim JH. Sliding mode control for trajectory tracking of non-holonomic wheeled mobile robots. *IEEE Trans Robot Autom* 1999; 15(3): 578–587.
4. Shiri R and Saeed RN. A general approach to dynamic gain adaptation of sliding mode control for robotic arms with parameter uncertainty. *Majlesi J Mechatron Syst* 2016; 5(4): 21–39.
5. Matveev AS, Hoy M, Katupitiya J, et al. Nonlinear sliding mode control of an unmanned agricultural tractor in the presence of sliding and control saturation. *Robot Auton Syst* 2013; 61(9): 973–987.
6. Sarfraz M, Rehman F and Shah I. Robust stabilizing control of non-holonomic systems with uncertainties via adaptive integral sliding mode: an underwater vehicle example. *Int J Adv Robot Syst* 2017; 14(5): 1–11.
7. Guo Y and Woo PY. An adaptive fuzzy sliding mode controller for robotic manipulators. *IEEE Trans Syst Man Cybern A* 2003; 33(2): 149–160.
8. Son NN, Anh HPH and Truong DC. Inverse kinematics solution for robot manipulator based on adaptive MIMO neural network model optimized by hybrid differential evolution algorithm. In: *Proceedings of the 2014 international conference on robotics and biomimetics (IEEE-ROBIO-14)*, Bali, Indonesia, December 2014, pp. 2019–2024. IEEE.
9. Fei J and Lu C. Adaptive sliding mode control of dynamic systems using double loop recurrent neural network structure. *IEEE Trans Neural Network Learn Syst* 2017; 6: 1–12.
10. Akbarzadeh T and Shahnazi R. Direct adaptive fuzzy PI sliding mode control for a class of uncertain nonlinear systems. *IEEE Int Conf Syst Man Cybern* 2005; 3: 2548–2553.
11. Shahnazi R, Shanechi H, and Pariz N. Position control of induction and DC servomotors: a novel adaptive fuzzy PI sliding mode control. *IEEE Transactions on Energy Conversion* 2008; 23(1): 138–147.
12. Medhaffar H, Derbel N, and Damak T. A decoupled fuzzy indirect adaptive sliding mode controller with application to robot manipulator. *Int J Modell Identificat Control* 2006; l(l): 23–29.
13. Lin CM and Hsu CF. Adaptive fuzzy sliding-mode control for induction servomotor systems. *IEEE Trans Energy Convers* 2004; 19(2): 362–368.
14. Ho HF, Wong YK, and Rad AB. Adaptive fuzzy sliding mode control design: Lyapunov approach. In: *Proceeding of the 5th Asian control conference*, Vol. 3, 2004, pp. 1502–1507. IEEE xplore digital library.
15. Soltanpour MR, Khooban MH, and Khalghani MR. An optimal and intelligent control strategy for a class of nonlinear systems: adaptive fuzzy sliding mode. *J Vibrat Control* 2016; 22(1): 159–175.
16. Anand R and Mary PM. Improved dynamic response of DC to DC converter using hybrid PSO tuned fuzzy sliding mode controller. *Circuits Syst* 2016; 7(6): 946.
17. Wang Y and Fei J. Adaptive fuzzy sliding mode control for PMSM position regulation system. *Int J Innov Comput Inf Control* 2015; 11(3): 881–891.
18. Ullah N, Shaoping W, Khattak MI, et al. Fractional order adaptive fuzzy sliding mode controller for a position servo system subjected to aerodynamic loading and nonlinearities. *Aerosp Sci Technol* 2015; 43: 381–387.
19. Oveisi A and Nestorović T. Robust observer-based adaptive fuzzy sliding mode controller. *Mech Syst Sig Proc* 2016; 76: 58–71.
20. Boldbaatar EA and Lin CM. Self-learning fuzzy sliding-mode control for a water bath temperature control system. *Int J Fuzzy Syst* 2015; 17(1): 31–38.
21. Moussaoui S and Abdesselem B. Stable adaptive fuzzy sliding-mode controller for a class of underactuated dynamic systems. In: *Conference on recent advances in electrical engineering and control applications. Springer International Publishing*, 2017, Vol. 411, pp. 114–124. LNEE.
22. Fei J and Xin M. An adaptive fuzzy sliding mode controller for MEMS tri-axial gyroscope with angular velocity estimation. *Nonlinear Dyn* 2012; 70(1): 97–109.
23. Jiao X and Ju J. Design of interval type-2 fuzzy sliding mode controller for hypersonic aircraft. *J Autom Control Eng* 2016; 4(2): 123–126.
24. Li H, Wang J, Lam HK, et al. Adaptive sliding mode control for interval type-2 fuzzy systems. *IEEE Trans Syst Man Cybern Syst* 2016; 46(12): 1654–1663.
25. Liang X, Wan L, Blake JI, et al. Path following of an underactuated AUV based on fuzzy backstepping sliding mode control. *Int J Adv Robot Syst* 2016; 13(3): 1–11.
26. Amar R, Mustapha H, and Mohamed T. Decentralized RBFNN type-2 fuzzy sliding mode controller for robot manipulator driven by artificial muscles. *Int J Adv Robot Syst* 2012; 9(5): 182, 1–12.
27. Chang MK. An adaptive self-organizing fuzzy sliding mode controller for a 2-DOF rehabilitation robot actuated by pneumatic muscle actuators. *J Cont Eng Pract* 2010; 18: 13–22.
28. Shi GL and Shen W. Hybrid control of a parallel platform based on pneumatic artificial muscles combining sliding mode controller and adaptive fuzzy CMAC. *Control Eng Pract* 2013; 21(1): 76–86.